

New Journal of Chemistry

Supporting Information

Luminescent diphosphine fluorophenylthiolate silver(I) compounds that exhibit argentophilic interactions

G. Moreno-Alcántar ^a, A. Nácar ^a, M. Flores-Álamo ^a and H. Torrens ^a.

^aDivisión de Estudios de Posgrado, Facultad de Química, UNAM, Ciudad Universitaria, 04510 México D.F., Mexico.

Experimental Details

Synthesis of silver thiolates (AgSR_F)

To a dissolution of 169.9 mg (1 mmol) of AgNO₃ in water (10 mL) 146.0 mg (1 mmol) of the difluorophenithiol dissolved in ethanol was added, the resultant mixture was stirred for 1 hour at room temperature. A pale yellow precipitate was filtered and washed with H₂O:EtOH 1:1 (10 mL x 2).

Procedures for preparation of compounds.

Compounds 1A [Ag₂(μ-3,4-dfbt)₂(dppBz)₂] and **1B** [Ag₂(μ-3,5-dfbt)₂(dppBz)₂] 446.5 mg (1.0 mmol) of 1,2-bis(diphenylphosphine)benzene were mixed with a suspension of 253 mg (1.0 mmol) of the corresponding silver difluorophenylthiolate in CH₂Cl₂ (25 mL) and resulting mixture was stirred by 24 hours at room temperature. The obtained uncolored solution volume was reduced to 5 mL then about 15 mL of hexane were added and white precipitate appears.

Compounds 2A [Ag₂(μ-3,4-dfbt)₂(dppE)₂] and **2B** [Ag₂(μ-3,5-dfbt)₂(dppE)₂] 396.4 mg (1.0 mmol) of 1,2-bis(diphenylphosphine)ethylene were mixed with a suspension of 253 mg (1.0 mmol) of the corresponding silver difluorophenylthiolate in CH₂Cl₂ (25 mL) and resulting mixture was stirred by 24 hours at room temperature. The obtained uncolored solution volume was reduced to 5 mL then about 15 mL of hexane were added and white precipitate appears.

Instrumental information: IR spectra were collected in a spectrometer Perkin-Elmer FTIR / FIR Spectrum 400 from 4000 to 400 cm⁻¹ by Attenuated total reflection (ATR); RMN spectra were obtained in a 9.4 T RMN (400 MHz) spectrometer Varian VNMRs. Mass spectra; FAB + spectra were measured in a mass spectrometer JEOL The MStation JMS-700. XRPD was measured in a Bruker D2 PHASER diffractometer figures of single crystal and powder X-ray diffraction patterns are shown for each compound, Match! software was used in processing. Solid state RT emission spectra were obtained in a Horiba

FluoroMax 4 Spectrofluorometer, in all cases excitation was made at 310 nm with 1 nm slit bandpass. Elemental analyses were determined using a Perkin Elmer 240 analyzer.

Compound 1A $[\text{Ag}_2(\mu\text{-3,4-dfbt})_2(\text{dppBz})_2]$ was obtained as white powder in 81% yield; m.p. 223-226 °C; IR $\nu_{\text{max}}/\text{cm}^{-1}$ 3050w (CH), 1588 and 1489s (C-C ar), 1264.5vs and 1161s (C-F). ^1H NMR (400 MHz, Chloroform-d, Me_4Si) δ 7.98 (m, 1H), 7.63 (m 1H), 7.52 – 7.39 (m, 8H), 7.39 – 7.30 (m, 8H), 7.29 – 7.19 (m, 11H), 7.19 – 7.04 (m, 39H). ^{19}F NMR (376 MHz, Chloroform-d, CFCl_3) δ ^{19}F NMR (376 MHz, C_6D_6) δ -134.04 (m), -135.26 (m), ^{31}P NMR (162 MHz, Chloroform-d, H_3PO_4) δ -0.55(br s), -10.40 (br s). FAB+ m/z 1001 ($[\text{Ag}(\text{dppBz})_2]^+$, 55%), 807 ($\text{M}^+ - [\text{dppBz} - \text{dfbt}]$, 5), 553 ($[\text{Ag}(\text{dppBz})]^+$, 100), 395 ($[\text{Ag}(\text{dfbt})_2]^+$, 10). Anal. % calcd. for $\text{C}_{72}\text{H}_{54}\text{Ag}_2\text{F}_4\text{P}_4\text{S}_2$: C, 61.82; H, 3.89; S, 4.58 found C, 60.93; H, 3.91; S, 4.43.

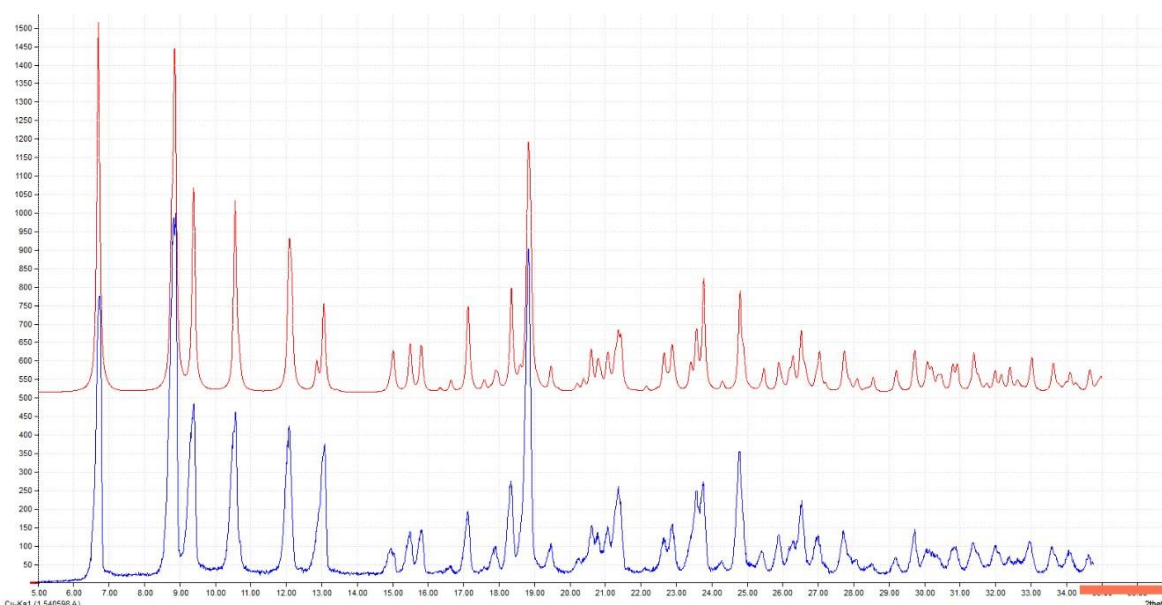


Fig 1. Crystal (top) and powder (down) X-Ray diffraction patterns for 1A

Compound 2A $[\text{Ag}_2(\mu\text{-3,4-dfbt})_2(\text{dppE})_2]$ was obtained as white powder in 78% yield; m.p. 135-139 °C; IR $\nu_{\text{max}}/\text{cm}^{-1}$ 3051w (CH), 1587s, 1487vs and 1433s (C-C ar), 1263.5vs and 1188s (C-F). ^1H NMR (400 MHz, Chloroform-d, Me_4Si) δ 7.53 – 7.37 (m, 2H), 7.37 – 7.13 (m, 40H), 6.96 – 6.79 (m, 4H), 6.15 (dd br, 4H CH=CH). ^{19}F NMR (376 MHz, Chloroform-d, CFCl_3) δ -133.44 (m), -134.80(m), ^{31}P NMR (162 MHz, Chloroform-d, H_3PO_4) δ -8.0 – -16.(br s). FAB+ m/z 901 ($[\text{Ag}(\text{dppE})_2]^+$, 30%), 757 ($\text{M}^+ - [\text{dppE} - \text{dfbt}]$, 7), 503 ($[\text{Ag}(\text{dppE})]^+$, 100), 395 ($[\text{Ag}(\text{dfbt})_2]^+$, 12). Anal. % calcd. for $\text{C}_{72}\text{H}_{54}\text{Ag}_2\text{F}_4\text{P}_4\text{S}_2$: C, 61.82; H, 3.89; S, 4.58 found C, 62.79; H, 3.96; S, 4.51.

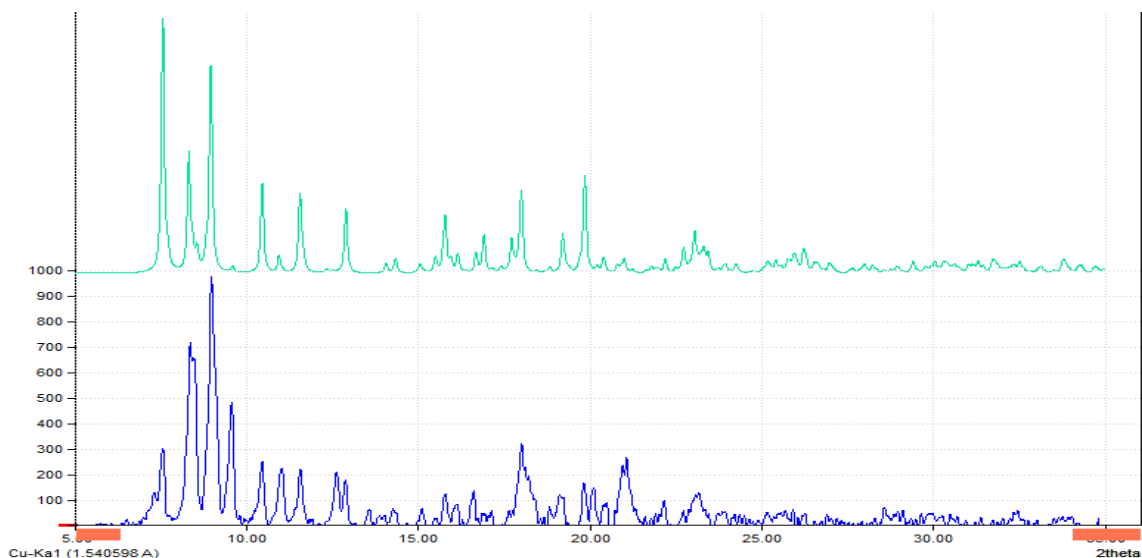


Fig 2. Crystal (top) and powder (down) X-Ray diffraction patterns for 2A

Compound 1B $[\text{Ag}_2(\mu\text{-}3,5\text{-dfbt})_2(\text{dppBz})_2]$ was obtained as white powder in 83% yield; m.p. 208-210 °C; IR $\nu_{\text{max}}/\text{cm}^{-1}$ 3052w (CH), 1600vs, 1574vs and 1435s (C-C ar), 1108vs (C-F). ^1H NMR (400 MHz, Chloroform-d, Me_4Si) δ 7.61 – 6.85 (m, 52H), 6.11 (t, $J = 9.1$ Hz, 2H). ^{19}F NMR (376 MHz, Chloroform-d, CFCl_3) δ -108.25 (dd, $J = 8.5, 6.1$ Hz). ^{31}P NMR (162 MHz, Chloroform-d, H_3PO_4) δ -0.78 (s br), -9.96 (s br). FAB+ m/z 1001 ($[\text{Ag}(\text{dppBz})_2]^+$, 60%), 807 ($\text{M}^+ - [\text{dppBz} - \text{dfbt}]$, 6), 553 ($[\text{Ag}(\text{dppBz})]^+$, 100), 395 ($[\text{Ag}(\text{dfbt})_2]^+$, 10). Anal. % calcd. for $\text{C}_{72}\text{H}_{54}\text{Ag}_2\text{F}_4\text{P}_4\text{S}_2$: C, 61.82; H, 3.89; S, 4.58 found C, 60.45; H, 3.86; S, 4.65.

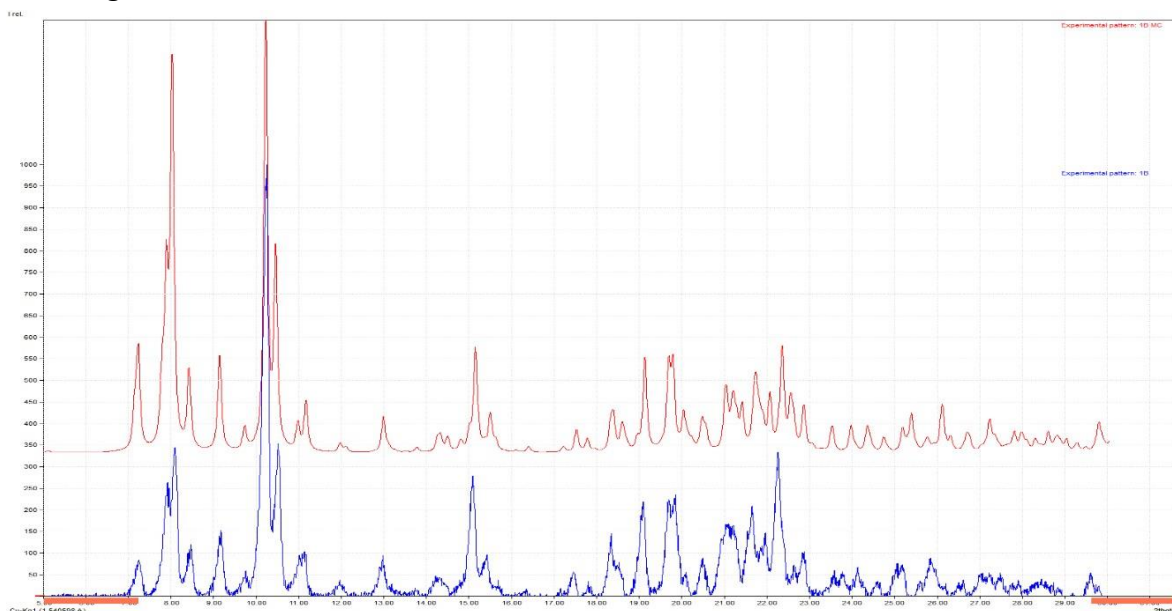


Fig 3. Crystal (top) and powder (down) X-Ray diffraction patterns for 1B

Compound 2B $[\text{Ag}_2(\mu\text{-}3,5\text{-dfbt})_2(\text{dppE})_2]$ was obtained as white powder in 79% yield; m.p. 150-153°C; IR $\nu_{\text{max}}/\text{cm}^{-1}$ 3052w (CH), 1598s, 1576w and 1488s (C-C ar), 1109s (C-F). ^1H NMR (300 MHz, Chloroform-d, Me_4Si) δ 7.53 – 6.79 (m, 46H), 6.35 (s br, 2H), 6.12 (m, 4H

CH=CH) ^{19}F NMR (376 MHz, Chloroform-d, CFCl_3) δ -112.15 (m). ^{31}P NMR (162 MHz, Chloroform-d, H_3PO_4) δ -8.45(br s), -14.6 (br s). FAB+ m/z 901 ($[\text{Ag}(\text{dppE})_2]^+$, 28%), 757 ($\text{M}^+ - [\text{dppE} - \text{dfbt}]$, 9), 503 ($[\text{Ag}(\text{dppE})]$, 100), 395 ($[\text{Ag}(\text{dfbt})_2]$, 8). Anal. % calcd. for $\text{C}_{72}\text{H}_{54}\text{Ag}_2\text{F}_4\text{P}_4\text{S}_2$: C, 61.82; H, 3.89; S, 4.58 found C, 61.12; H, 3.87; S, 4.69.

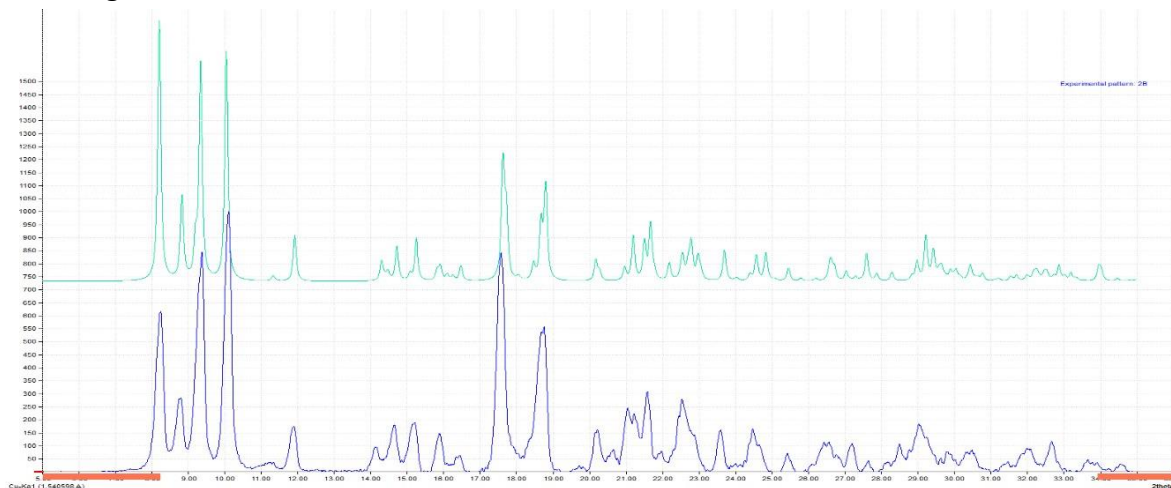


Fig 4. Crystal (top) and powder (down) X-Ray diffraction patterns for 2B

Note: ^{31}P NMR spectra shows in all cases broad signals which are due to mixed species in equilibrium in combination with heteronuclear couplings with Ag and ^1H . Further low temperature studies are needed to precisely determine shift and coupling constants.

[1]

Luminescence of compounds.

Diffuse reflectance absorption spectra for compounds is showed in figure 5, all compounds show broad absorption bands from 250 to 350 nm which seems to be composed of the reported ligand absorption (260 nm) but it has another important contribution above 300 nm. It is notable that compounds 1A and 1B displayed negative reflectance values in the region of 440 to 550 nm due to the strong emission.

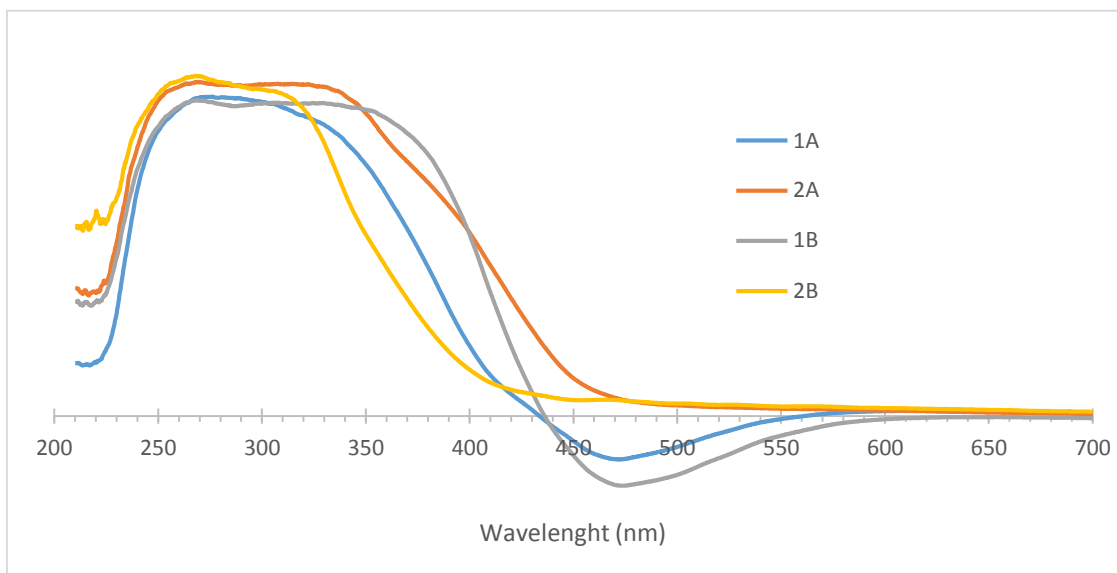


Fig 5. Absorption spectra for the four compounds obtained by diffuse reflectance.

Emission spectra of compounds is shown in figure 6, in relation with previously reported emission for homoleptic $[\text{Ag}(\text{dppBz})_2]\text{NO}_3$ with a $\lambda_{\text{max}}=445$ nm we observe a red shifted emission.

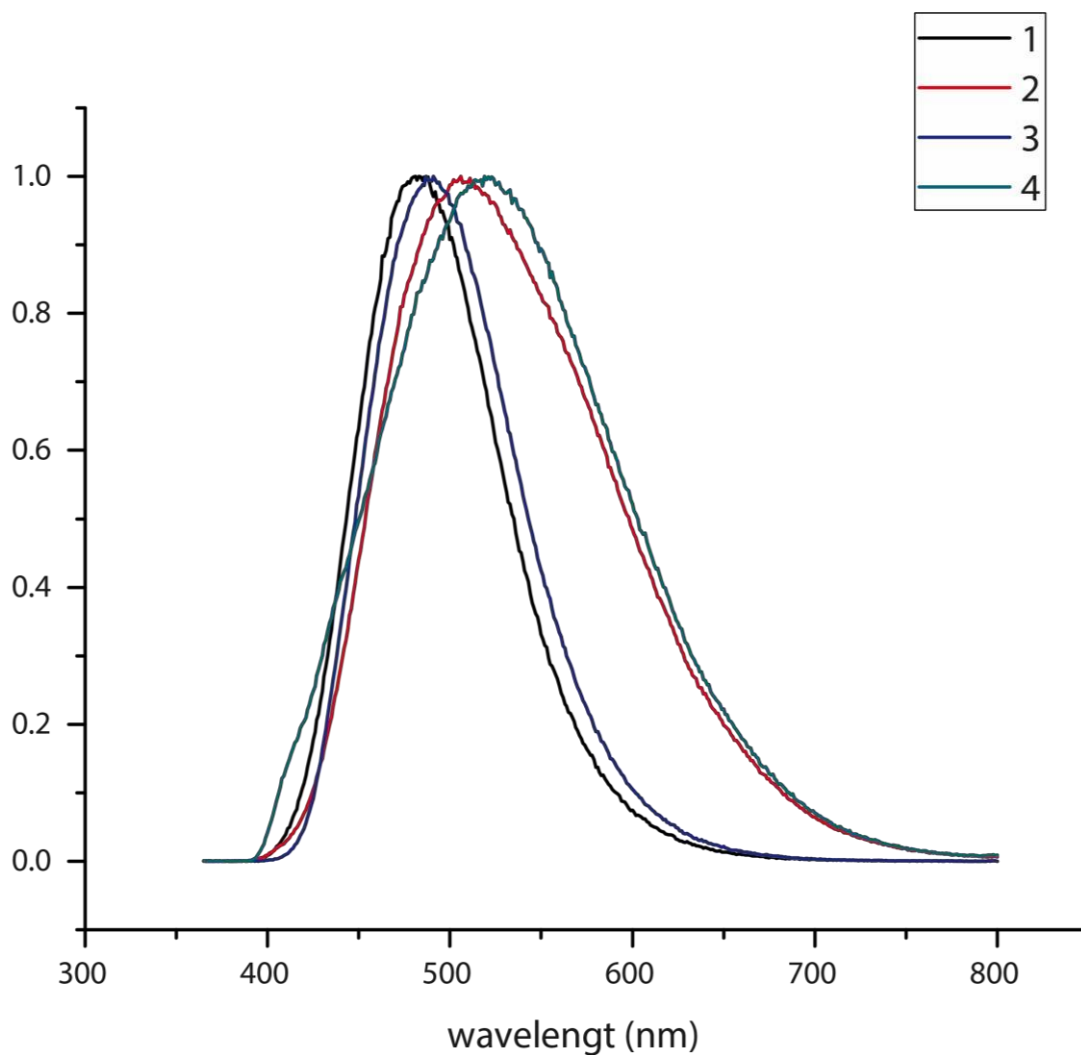


Fig 6. Emission spectra of compounds 1A(1), 2A(2), 1B(3) and 2B(4).

X-ray crystallography.

A suitable single crystals of **1A**, **1B**, **2A** and **2B** were mounted on a glass fiber and studied with an Oxford Diffraction Gemini "A" diffractometer with a CCD area detector, with radiation source of $\lambda_{MoK\alpha} = 0.71073 \text{ \AA}$ using graphite-monochromatized radiation at 298K for **1A** and **2A**, and 130 K for **1B** and **2B**. Unit cell parameters were determined with a set of three runs of 15 frames (1° in ω). The collected data set consisted of 4/265, 7/503, 6/507 and 13/1008 runs/frames of intensity (1° in ω) for **1A**, **1B**, **2A** and **2B** respectively, and a crystal-to-detector distance of 55.00 mm. The double pass method of scanning was used to exclude any noise. The collected frames were integrated by using an orientation matrix determined from the narrow frame scans.

CrysAlisPro and CrysAlis RED software packages were used for data collection and integration [2]. The double pass method of scanning was used to exclude any noise. The collected frames were integrated by using an orientation matrix determined from the narrow frame scans. Final cell constants were determined by a global refinement; collected data were corrected for absorbance by using analytical numeric absorption correction using a multifaceted crystal model based on expressions upon the Laue symmetry using equivalent reflections [3]. Structure solution and refinement were carried out with the SHELXS-2014 and SHELXL-2014 packages [4]; WinGX v2014.1 software was used to prepare material for publication [L. J. Farrugia, *Appl. Cryst.*, 1999, **32**, 837–838].

Full-matrix least-squares refinement was carried out by minimizing $(F_o^2 - F_c^2)^2$. All nonhydrogen atoms were refined anisotropically and the refinement was carried out without restraint. Hydrogen atoms attached to carbon atoms were placed in geometrically idealized positions and refined as riding on their parent atoms, with C—H = 0.93 – 095 Å with Uiso (H) = 1.2Ueq(C) for methylene, methyne and aromatic groups.

Crystal data and experimental details of the structure determination are listed in Table SI-1.

Table SI-1. Crystal data and structure refinement for of **1A**, **1B**, **2A** and **2B** compounds.

Identification code	1A	1B	2A	2B
Empirical formula	C ₇₂ H ₅₄ Ag ₂ F ₄ P ₄ S ₂	C ₇₂ H ₅₄ Ag ₂ F ₄ P ₄ S ₂	C ₆₄ H ₅₀ Ag ₂ F ₄ P ₄ S ₂	C ₆₄ H ₅₀ Ag ₂ F ₄ P ₄ S ₂
Formula weight	1398.89	1398.89	1298.78	1298.78
Temperature (K)	298(2)	130(2)	298(2)	130(2)
Wavelength (Å)	0.71073	0.71073	0.71073	0.71073
Crystal system	Monoclinic	Triclinic	Triclinic	Triclinic
Space group	P 21/n	P -1	P -1	P -1
Crystal size (mm ³)	0.240 x 0.100 x 0.060	0.330 x 0.210 x 0.120	0.440 x 0.390 x 0.250	0.580 x 0.540 x 0.410
a (Å)	a = 14.1703(7)	a = 13.8314(8)	a = 11.7331(4)	a = 11.8531(7)
b (Å)	b = 10.6446(5)	b = 13.9584(12)	b = 11.9626(4)	b = 11.9647(7)
c (Å)	c = 21.0933(10)	c = 18.0610(11)	c = 21.2821(6)	c = 12.1327(7)
α (°)	α = 90	α = 73.771(6)	α = 92.527(2)	α = 64.180(5)
β (°)	β = 107.068(5)	β = 78.567(5)	β = 92.533(2)	β = 65.204(6)
γ (°)	γ = 90	γ = 63.638(7)	γ = 102.148(3)	γ = 81.877(5)
Volume (Å ³)	3041.5(3)	2988.7(4)	2913.02(16)	1404.27(16)
Z	2	2	2	1
ρ _{calc} (Mg/m ³)	1.527	1.554	1.481	1.536
μ (mm ⁻¹)	0.874	0.889	0.906	0.940
F(000)	1416	1416	1312	656
θ range (°)	3.434 to 29.453	3.407 to 29.527	3.447 to 29.650	3.510 to 29.488
Index ranges	-17<=h<=19, - 14<=k<=12, -26<=l<=26	-18<=h<=18, - 19<=k<=18, -24<=l<=22	-16<=h<=16, - 15<=k<=15, -27<=l<=28	-16<=h<=15, - 16<=k<=16, -16<=l<=16
Reflections collected	20947	40130	39153	37061
Independent reflections	7278 [R(int) = 0.0440]	14460 [R(int) = 0.0309]	14065 [R(int) = 0.0315]	7186 [R(int) = 0.0295]
Completeness to theta = 25.242°	99.8 %	99.7 %	99.7 %	99.7 %
Refinement	Full-matrix least-squares on F ²	Full-matrix least-squares on F ²	Full-matrix least-squares on F ²	Full-matrix least-squares on F ²
Data / restr / parameters	7278 / 0 / 388	14460 / 0 / 757	14065 / 0 / 685	7186 / 0 / 343
Goodness-of-fit on F ²	1.017	1.052	1.031	1.096
Final R indices [I>2σ(I)]	R1 = 0.0403, wR2 = 0.0640	R1 = 0.0319, wR2 = 0.0650	R1 = 0.0371, wR2 = 0.0696	R1 = 0.0226, wR2 = 0.0566
R indices (all data)	R1 = 0.0842, wR2 = 0.0780	R1 = 0.0452, wR2 = 0.0723	R1 = 0.0643, wR2 = 0.0814	R1 = 0.0262, wR2 = 0.0587
Largest diff. peak and hole	0.336 and -0.576 e.Å ⁻³	0.946 and -0.712 e.Å ⁻³	0.480 and -0.491 e.Å ⁻³	0.526 and -0.594 e.Å ⁻³

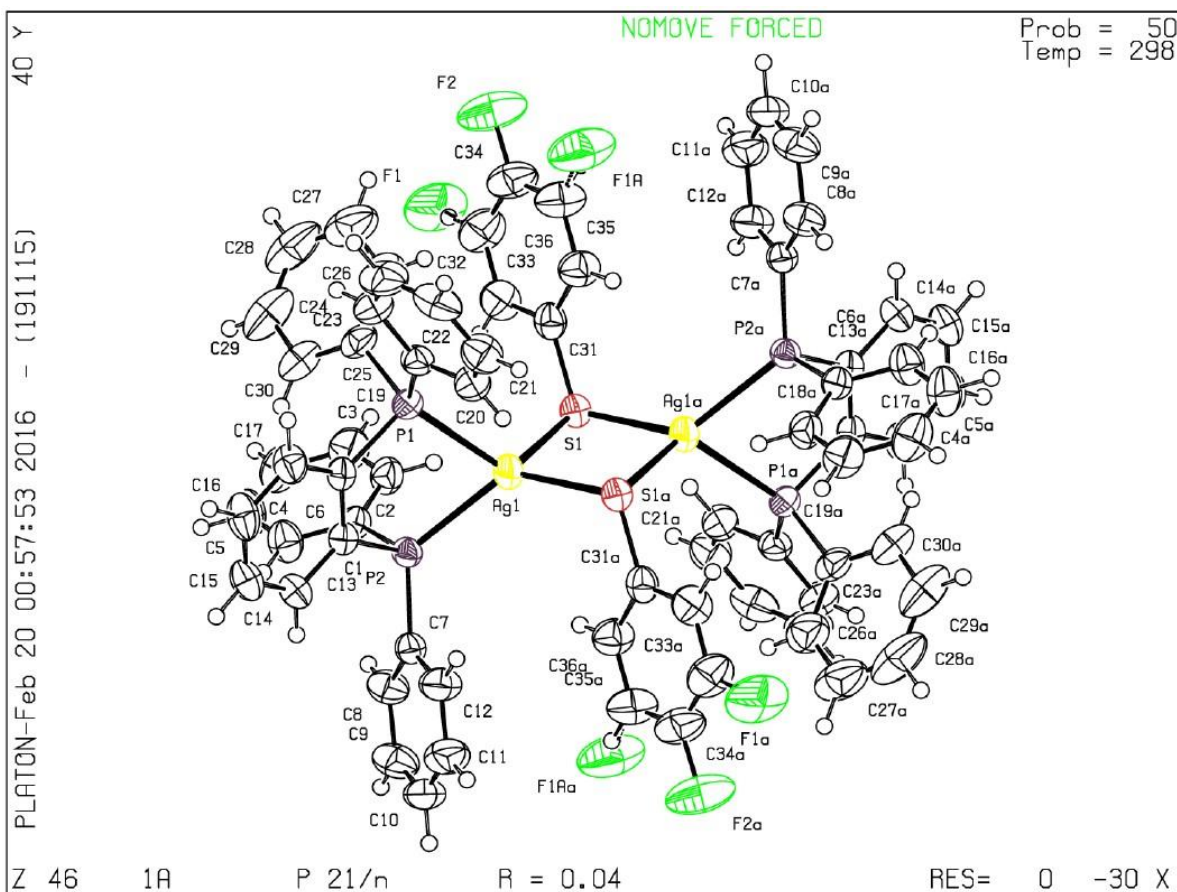


Fig 7 ORTEP plot at 50% probability level for compound 1A.

In compound 1A x-ray structure, we found fluorine F1 disordered over two positions with occupancies of 0,75 (F1A) and 0,25(F1) analyzing the structure we observe that both positions give to the fluorine atom the possibility of form H-bonds with hydrogens attached at peripheral phenyl rings (Fig 7).

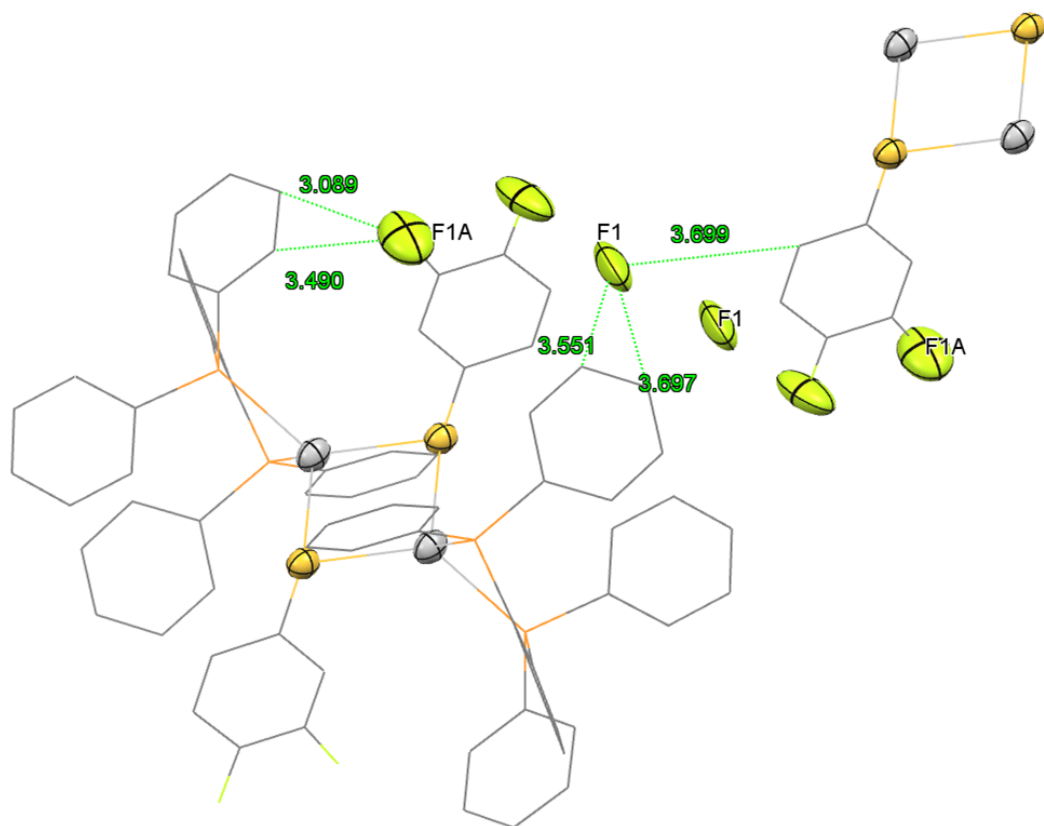


Fig 8. H-bonds formed in each of two possible fluorine F1 positions which are responsible of the observed disorder.

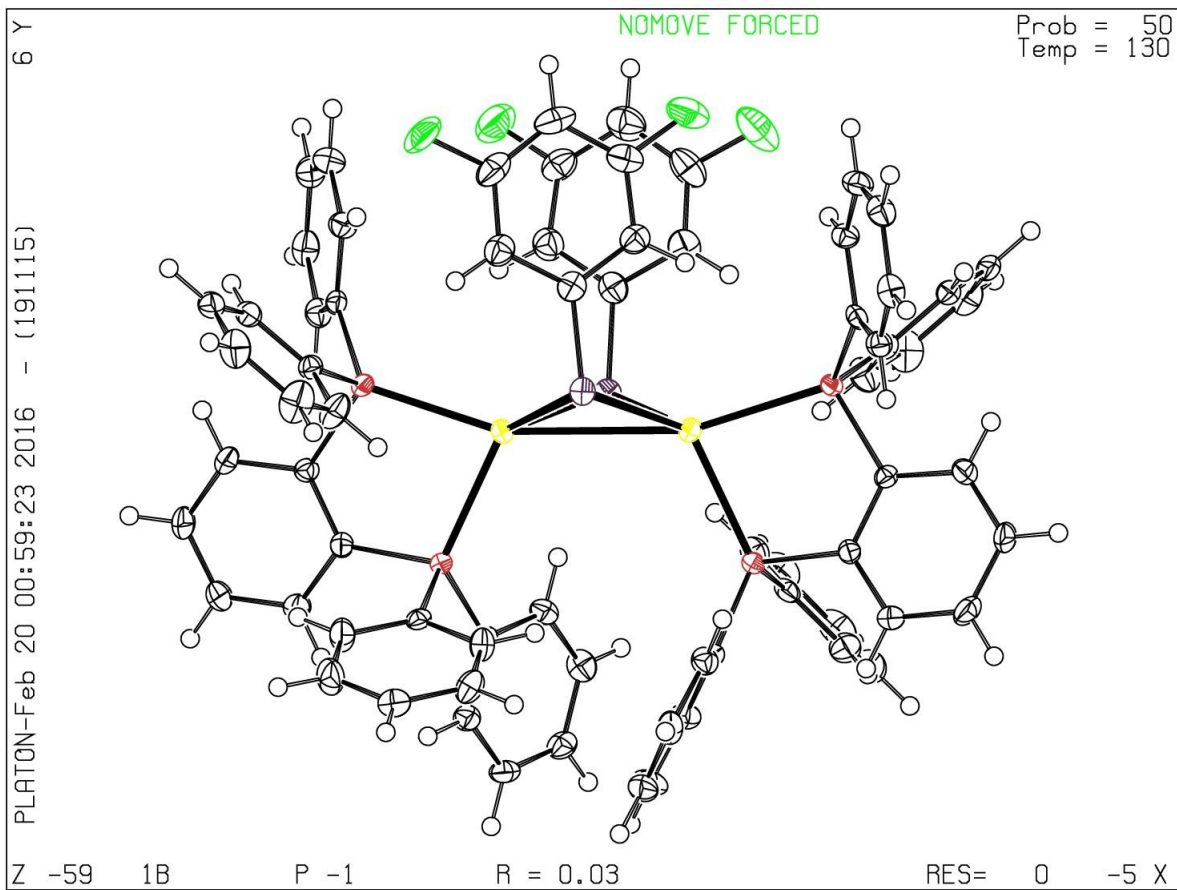


Fig 9. ORTEP plot at 50% probability level for compound 1B.

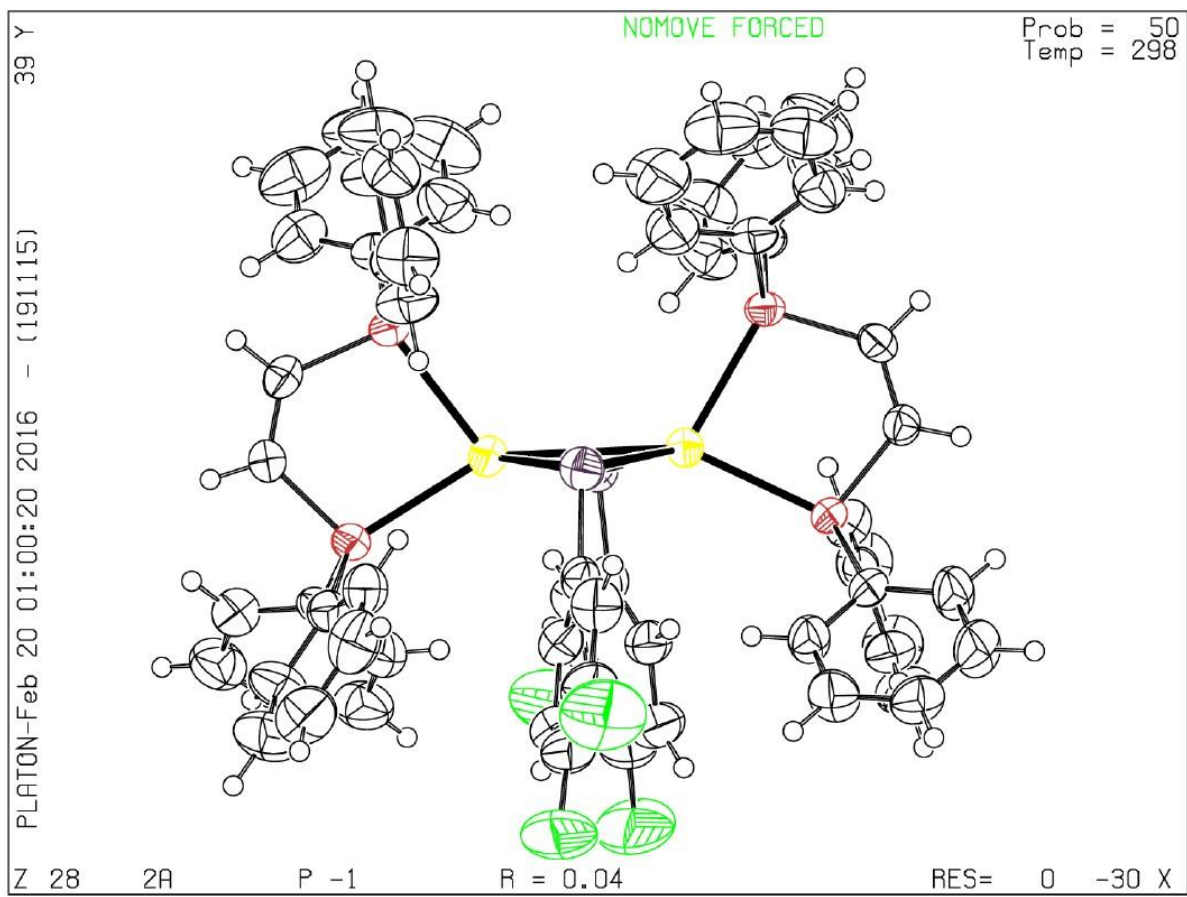


Fig 10. ORTEP plot at 50% probability level for compound 2A.

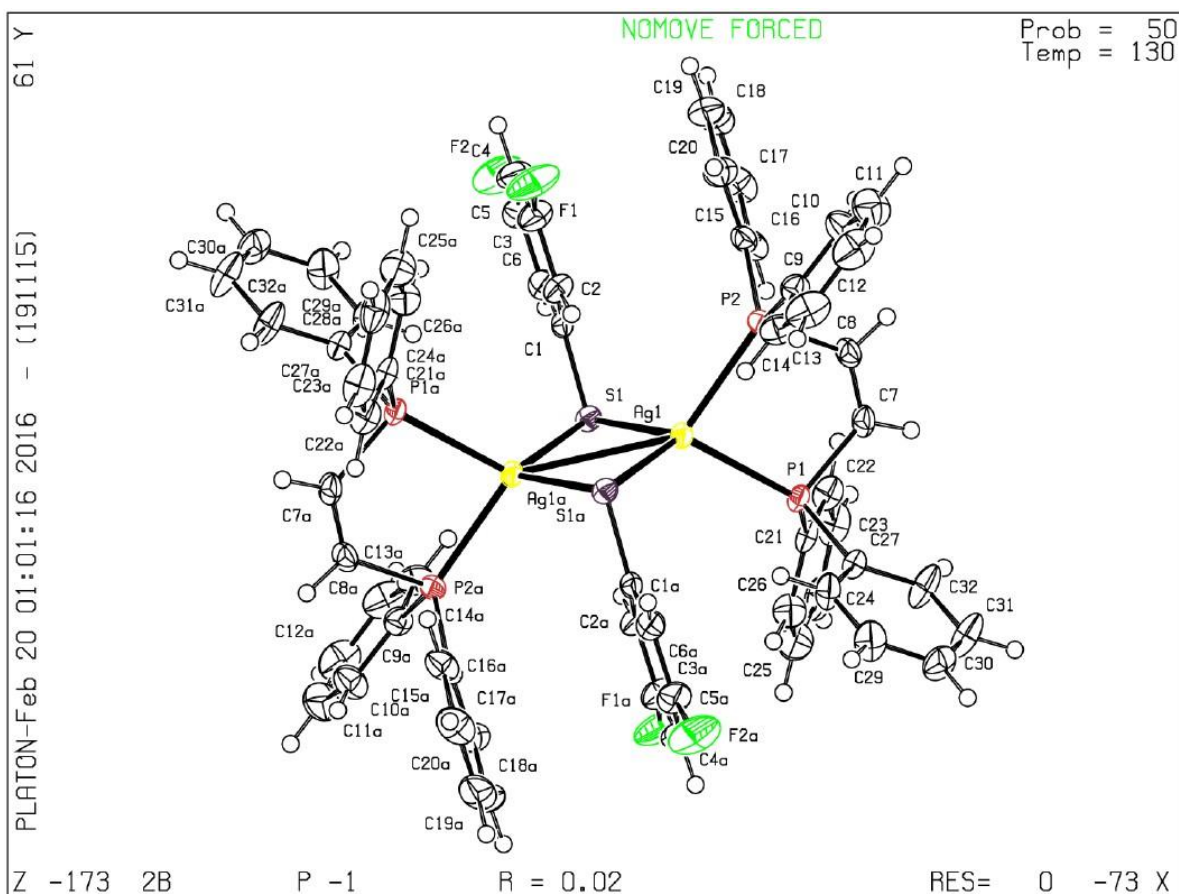


Fig 11. ORTEP plot at 50% probability level for compound 2B.

- [1] X. L. Lu, W. K. Leong, T. S. A. Hor and L. Y. Goh, *J. Organomet. Chem.*, 2004, **689**, 1746–1756.
- [2] Agilent (2013). *CrysAlis PRO* and *CrysAlis RED*. Agilent Technologies, Yarnton, England
- [3] R. C. Clark and J. S. Reid, *Acta Cryst.*, 1995, **A51**, 887–897
- [4] G. M. Sheldrick, *Acta Cryst.*, Sect. A: Found. Crystallogr., 2008, **64**, 112–122